Broadband absorption and light-energy transfer in a phenyl-core thiophene dendrimer with multiple π-conjugations

Yamagishi, Mizuho
Horike, Shohei
Koshiba, Yasuko
Mori, Atsunori
Ishida, Kenji

(Citation)
Molecular Systems Design & Engineering,8(2):189-194

(Issue Date)
2023-02-01

(Resource Type)
journal article

(Version)
Version of Record

(URL)
https://hdl.handle.net/20.500.14094/0100479014

MSDE

PAPER

View Article Online
View Journal | View Issue

Cite this: *Mol. Syst. Des. Eng.*, 2023, **8**, 189

Received 27th July 2022,
Accepted 13th December 2022

DOI: 10.1039/d2me00157h

rsc.li/molecular-engineering

Broadband absorption and light-energy transfer in a phenyl-core thiophene dendrimer with multiple π-conjugations†

Mizuho Yamagishi,[a] Shohei Horike,[abc] Yasuko Koshiba,[ab]
Atsunori Mori[ab] and Kenji Ishida *[ab]

π-Conjugated dendrimers, with unique optical properties, have the potential to be used as light-harvesting antenna in organic solar cells and photodetectors. Here, the broadband absorption and light-energy transfer in a phenyl-core thiophene dendrimer, Ph-$(7T)_3$, have been investigated using quantum calculations and absorption, photoluminescence, and excitation spectroscopy. The broadband absorption of the highly branched Ph-$(7T)_3$ macromolecule could be attributed to multiple π-conjugations in Ph-$(7T)_3$ (due to phenylthiophene and thiophene oligomers with different numbers of thiophene units). The divergency of the wavelengths between photoluminescence and excitation light indicated that the multiple π-conjugating system exhibited various modes of excited-state relaxation, which could explain the light-energy transfer from the core to the thiophene dendrons. The fluorescent quantum yield and lifetime of this molecular system are also presented.

Design, System, Application

π-Conjugated dendrimers offer significant advantages in opt-electronic applications owing to the customizability of their highly branched molecular systems and functions that can be realized by designing each π-conjugation moiety for the desired properties. In this study, the photochemistry of a phenyl-core thiophene dendrimer, developed with various π-conjugation patterns, was investigated *via* the complementary characterization of quantum calculation and absorption, photoluminescence, and excitation spectroscopy. Owing to the combination of the multiple π-conjugations, the dendrimer exhibited unique broadband absorption and light-energy transfer from the core to the thiophene dendrons. The results of this study demonstrated that a combination of quantum calculations and spectroscopy for each part of the dendrimer can be used as an effective baseline to synthesize π-conjugated dendrimers with specific properties. Thus, they can provide a basis for the development of a novel class of optoelectronic materials.

1. Introduction

Dendrimers are branched macromolecules that consist of dendrons attached to a core.[1–6] Dendrimers exhibit several advantages compared with typical linear-shaped polymers, such as, well-defined molecular weights, good batch-to-batch reproducibility, and molecular design tunability.[7–12] Furthermore, high-generation dendrimers exhibit spherical molecular morphology that enables the introduction of functional groups on the molecular surface. Thus, dendrimers exhibit immense potential as functional materials in the fields of medical science[13–17] and organic chemistry.[18–22]

Recently, the structural advantages and unique physicochemical properties of dendrimers have been utilized in various research fields; dendrimers with rigid π-conjugated backbones have been extensively studied as a new class of optical and electronic materials.[23–25] Benzyl ether dendrimers containing azobenzene transfer infrared absorption energy in the aromatic unit to the core azobenzene.[24] Furthermore, the light-harvesting ability of phenylacetylene dendrimers has been characterized by electroluminescence using the light-emitting-diode configuration.[25] The light-harvesting properties of dendrimers could be utilized in light-emitting and photoelectric devices.

Additionally, the optoelectronic and electronic properties of thiophene-containing dendrimers have attracted immense attention[26–28] because thiophene oligomers and polymers exhibit efficient charge-transport properties and electronic-

---

[a] *Department of Chemical Science and Engineering, Graduate School of Engineering, Kobe University, 1-1 Rokkodai-cho, Nada-ku, Kobe, 657-8501, Japan. E-mail: kishida@crystal.kobe-u.ac.jp*

[b] *Research Center for Membrane and Film Technology, Kobe University, 1-1 Rokkodai-cho, Nada-ku, Kobe, 657-8501, Japan*

[c] *PRESTO, Japan Science and Technology Agency, Kawaguchi, 332-0012, Japan*

† Electronic supplementary information (ESI) available: Quantum calculations; photoluminescence spectra. See DOI: **https://doi.org/10.1039/d2me00157h**

state tunability *via* doping.[29,30] Usluer *et al.* have used thiophene dendrimers in organic light-emitting diodes;[31] the reported dendrimers exhibit heat resistance and reversible redox reactions. They have been used as hole-transporting layers in organic light-emitting diodes and exhibit green electroluminescence. Additionally, a fluorenyl hexa-*peri*-hexabenzocoronene (FHBC)-core dendrimer with thiophene dendrons synthesized by Wong *et al.* exhibits broadband ultraviolet-visible (UV-vis) absorption, unlike single FHBC molecules;[32] a BHJ solar cell with a light-to-electricity power conversion efficiency of 2.5% has been fabricated using a dendrimer-film stacked with a fullerene-derivative layer.

A comparison of the transition energies of π-conjugated dendrimers using absorption, photoluminescence (PL), and excitation spectroscopy could elucidate their photochemistry, including their excitation, light emission, vibrational relaxation, internal conversion, and internal crossing. Herein, the optical properties of a phenyl-core thiophene dendrimer, Ph-$(7T)_3$ (Fig. 1), have been investigated using quantum calculations and spectroscopic analyses.

The broadband absorption and wavelength-selective PL of Ph-$(7T)_3$ could be attributed to multiple π-conjugations existing in a single macromolecule (due to its branched chemical structure). The fluorescent quantum yield and lifetime of this molecular system are also presented. With the recent rapid progress in dendrimer synthesis, the measurements, analysis, and results described here could guide the design and development of π-conjugated dendrimers with desired optoelectronic functions.

2. Experimental

2.1. Chemicals

Ph-$(7T)_3$ with a purity of 96.32% was synthesized at the NARD Institute following a procedure reported by Tanaka *et al.*[33] $CHCl_3$, tetrahydrofuran (THF), hexane, toluene, and *N*-methyl-2-pyrrolidone (NMP) were purchased from Nacalai Tesque. All the chemicals were 99% pure and were used as received.

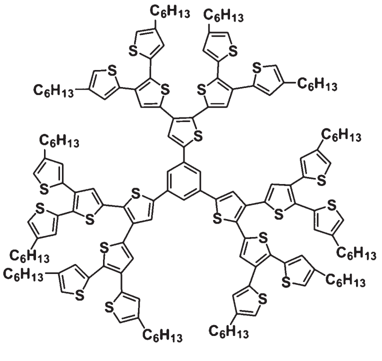

Fig. 1 Chemical structure of phenyl-core thiophene dendrimer, Ph-$(7T)_3$, consisting of three dendrons with seven thiophene rings (7T) branched from a core benzene. Letter "T" represents a thiophene ring.

2.2. Characterization

Ph-$(7T)_3$ was dissolved in $CHCl_3$, THF, hexane, toluene, and NMP at a concentration of 3.44×10^{-6} mol L^{-1}. The absorption spectra were recorded using a UV-vis spectrometer (V-670, JASCO), while the PL and excitation spectra were recorded using a fluorescence spectrometer (F-2500, HITACH). The fluorescence quantum yields and lifetime were recorded using an absolute PL quantum yield spectrometer equipped with an integrating sphere (C11347-01, Hamamatsu Photonics K. K.) and a picosecond laser (spectra-physics). The measurements were conducted at the Institute for Molecular Science, Japan. The quantum efficiency was calculated by dividing the peak area of PL from the sample by the difference between the peak areas of the excitation lights of the blank and sample measurements. A quartz-glass cell was used for all the measurements.

2.3. Quantum calculations

All quantum calculations were performed *via* density functional theory (DFT) using the Gaussian 3.0 package at the B3LYP/6-31G(d,p) GD3 level for geometry optimization, energy diagram simulation, and the mapping of the highest occupied molecular orbital (HOMO) and the lowest unoccupied molecular orbital (LUMO), and B3LYP/6-31G + (d, p) level for simulation of UV-vis spectra.

3. Results and discussion

3.1. Broadband absorption of Ph-$(7T)_3$ due to multiple π-conjugations

The synthesized Ph-$(7T)_3$ exhibited high solubility in common solvents due to the presence of hexyl groups. For example, it can be dissolved in $CHCl_3$, THF, hexane, toluene, and NMP while water, ethanol, and ethylene carbonate are not suitable as solvents. Each solution has a yellow color (Fig. 2a) and exhibits green emission (Fig. 2b) under UV light (375 nm). First, the UV-vis absorption spectrum of a $CHCl_3$ solution of Ph-$(7T)_3$ was recorded (Fig. 2c); broadband absorption was observed in the wavelength range of 250–510 nm. This class of broadband absorption is rarely seen in typical small-molecule organic semiconductors and could be attributed to the unique branched primary molecular structure of the dendrimer. Absorptions of the different moieties in Ph-$(7T)_3$ (*e.g.*, phenylthiophene, 1T, and 2T) contributed to its broadband absorption. The existence of such diverse electron-transition modes in a single molecule could be conceptualized as multiple π-conjugations.

To verify this concept, the absorption spectra originating from the 10 possible π-conjugation patterns in Ph-$(7T)_3$ (1T, 2T, 3T, 4T, 5T, Ph-1T, Ph-2T, Ph-3T), were calculated, as shown in Fig. 2d. Two isomers were considered for 2T and 3T each because connecting thiophene rings at the α–α and α–β positions form different conjugation patterns (here denoted as α/α and α/β, respectively). The calculated wavelength-dissolved molar-absorption-coefficient spectra for the

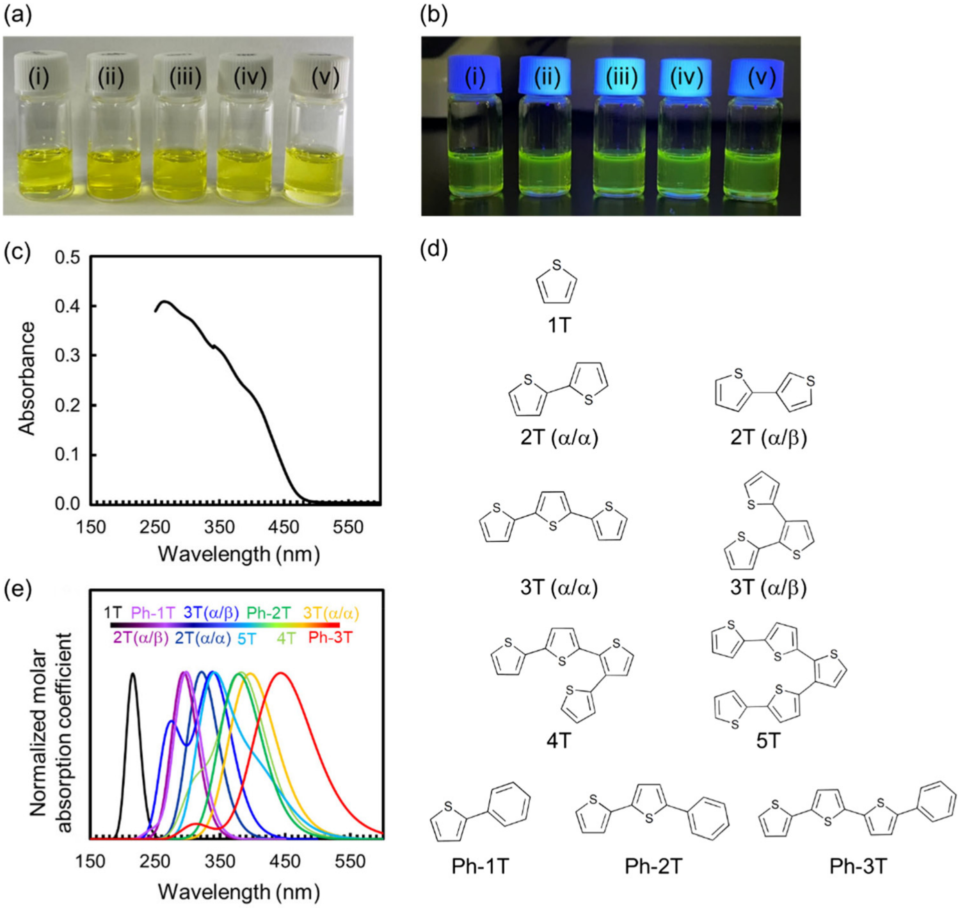

Fig. 2 Photos of Ph-(7T)$_3$ solutions (a) without UV irradiation and (b) under UV light at 375 nm. Solvents are (i) toluene, (ii) hexane, (iii) $CHCl_3$, (iv) THF, and (v) NMP. (c) Absorption spectrum of a $CHCl_3$ solution of Ph-(7T)$_3$; plots below the wavelength of 250 nm are excluded from the graph due to the strong absorption exhibited by the solvent (chloroform) in that wavelength region. (d) Chemical structures of 10 possible π-conjugation patterns included in Ph-(7T)$_3$. Two isomers are possible for 2T and 3T each due to head-to-head (HH) and head-to-tail (HT) bonding. Other moieties included in Ph-(7T)$_3$ are presented in Fig. S1 of the ESI.† (e) Simulated wavelength-dissolved molar-absorption-coefficient spectra of molecules shown in panel b. Spectra are normalized by peak-top values; absolute coefficient values, molecular orbital mappings, energy diagrams, and frontier molecular orbital energy levels are provided in Table S1, Fig. S2, S3, and Table S2 of ESI,† respectively.

molecules are shown in Fig. 2e. Extended π-conjugation facilitates the absorption of long-wavelength light. Notably, the experimentally observed absorption spectrum (250–510 nm) of Ph-(7T)$_3$ (Fig. 2c) encompassed almost all the

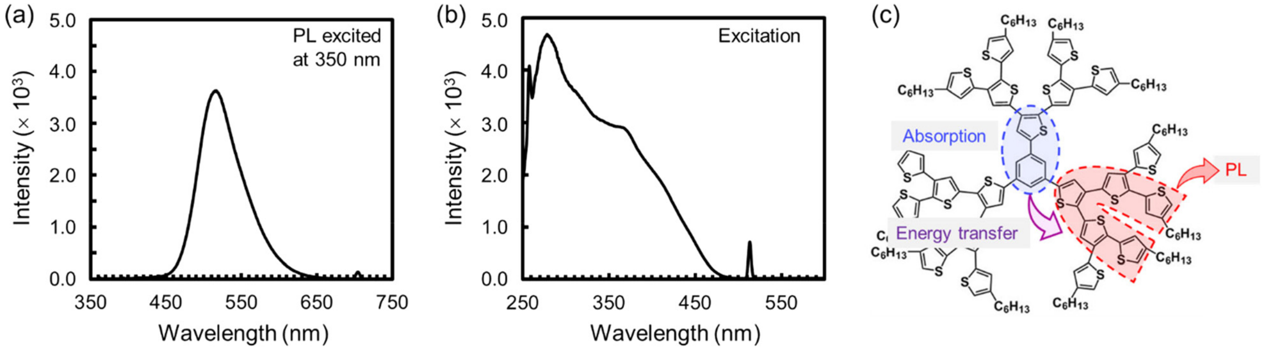

Fig. 3 (a) Photoluminescence (PL) spectrum of a $CHCl_3$ solution of Ph-(7T)$_3$ excited at 350 nm. (b) Excitation spectrum to induce PL with wavelength of 514 nm in $CHCl_3$ solution of Ph-(7T)$_3$. The sharp features at 514 and 257 nm could be attributed to direct beam of PL light and its secondary light, respectively. (c) A schematic representation of absorbed-light-energy transfer from Ph-1T to 5T, and subsequent PL emission in Ph-(7T)$_3$.

Table 1 Fluorescence quantum yields and lifetime of Ph-(7T)$_3$ and 5T

Sample	ϕ_F[a] (%)	τ_1[b] (ns)	τ_2[b] (ns)	A_1[c]	A_2[c]	B[c] (ns)
Ph-(7T)$_3$	4.5	0.85	0.63	1.0×10^3	2.1×10^4	1.8
5T[d]	28 ± 6	0.87 ± 0.09				

[a] ϕ_F: Fluorescence quantum yields. [b] τ_i: Fluorescence lifetime. [c] A_i, B: Fitting parameters. [d] From Colditz *et al.*[36]

simulated spectra (Fig. 2e), confirming that the broadband absorption spectrum of Ph-(7T)$_3$ originated from a combination of the multiple π-conjugations in Ph-(7T)$_3$.

3.2. Light-energy transfer in Ph-(7T)$_3$ indicated by photoluminescence and excitation spectra

The light energy absorbed by a molecule is generally converted to PL and thermal energy (molecular vibrations). The PL spectrum of a CHCl$_3$ solution of Ph-(7T)$_3$ was used to analyze the relaxation process of excited Ph-(7T)$_3$. Fig. 3a shows the PL spectrum at an excitation wavelength of 350 nm, with a single peak at 514 nm. The peak could be attributed to electronic transitions from the LUMO to the HOMO energy levels (corresponding to the bandgap energy) of Ph-(7T)$_3$ because it is consistent with the absorption onset wavelength (∼510 nm) shown in Fig. 2c. Notably, the peak positions did not change according to the excitation wavelength and solvent types, as described in details in Fig. S4 and S5 of the ESI.†

The excitation spectrum was analyzed to further investigate the Ph-(7T)$_3$ relaxation process. Excitation spectroscopy identifies the dominant excitation wavelength that induces PL at a specific wavelength. Fig. 3b shows the excitation spectrum for inducing PL at a wavelength of 514 nm. The excitation spectrum for inducing PL at 514 nm covers a wide range of wavelengths (260–480 nm). Interestingly, the efficiency of inducing PL at 514 nm is higher at the shorter wavelength range and takes significantly high values at the wavelength range of 260–320 nm. Unique relaxation processes possibly occur in the dendrimer for its PL emission at 514 nm (corresponding to the bandgap) after irradiation with short-wavelength light.

Absorptions in the wavelength range of 260–320 nm were mainly caused by 2T (both α/β and α/α), Ph-1T, and 3T (α/β), as shown in Fig. 2e; therefore, these absorptions could be effectively converted into PL at 514 nm. The divergence between the photon energies with wavelengths in the range of 260–320 nm and those at 514 nm may be converted to other energies, such as vibration and internal conversion in the molecules. Moreover, photons with 514 nm wavelength caused electronic transitions in 3T, 4T, 5T, and Ph-3T (Fig. 2e). Therefore, the light-energy absorbed at the 2T, Ph-1T, and 3T sites could be transferred to the other parts such as 3T, 4T, 5T, and Ph-3T while being utilized for internal conversions and molecular vibrations, and finally emitted as PL for excited-state deactivation. The LUMO energy levels of 2T, Ph-1T, and 3T are shallower or similar to those of 3T, 4T, 5T, and Ph-3T as shown in Fig. S3 and Table S2 of the ESI;† therefore, electron transfer from the light-absorbing sites to the emitting sites would be possible.

Ph-1T absorbed light at a wavelength of 272 nm, as shown in Fig. 2e, which is almost identical to the experimentally observed absorption maxima of Ph-1T (264 nm).[34] Additionally, it was experimentally observed that 5T emitted PL at a wavelength of 515 nm.[35] In particular, the absorbed energy at the phenyl-thiophene-core unit was possibly transferred to the dendron 5T, as shown schematically in Fig. 3c. This light-energy transfer from Ph-1T to the dendron-thiophene moieties could be labeled as "core-to-dendron light-energy transfer".

This class of energy transfer is an extremely unique photochemical property of π-conjugated dendrimers.[37–41] This study highlights an effective baseline for customizing the primary molecular structures of dendrimers to tune their optoelectronic functions.

Finally, we measured the fluorescence quantum yield (ϕ_F) and lifetime of Ph-(7T)$_3$ to further quantify the relaxation processes and compare them with those of 5T, as summarized in Table 1. The quantum yield (ϕ_F) of Ph-(7T)$_3$ in CHCl$_3$ is *ca.* 4.5%, which is lower than that of 5T (ref. 35 and 36) but close to that of thiophene dendrimers with similar molecular structures.[8] As shown in Table S3 of the ESI,† the solvent does not affect the yield.

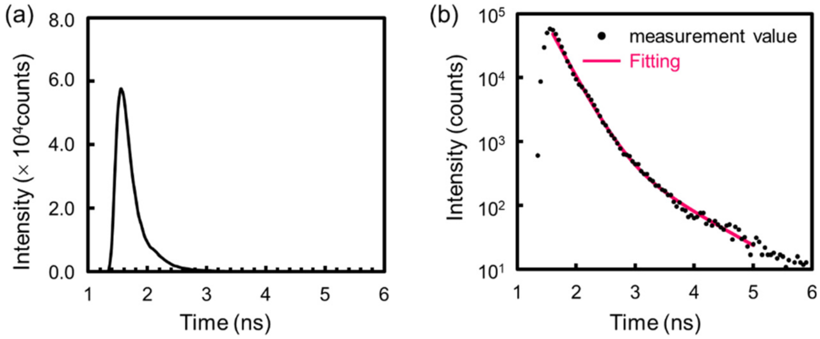

Fig. 4 (a) Decay profile of fluorescence of Ph-(7T)$_3$ in CHCl$_3$ at 514 nm recorded by excitation wavelength of 350 nm. (b) Logarithmic plot of decay profile shown in panel a. Red solid line represents a fitting curve.

As shown in Fig. 4a, the decay profile of fluorescence of the $CHCl_3$ solution of Ph-$(7T)_3$ shows a monotonic decrease. This could be fitted by a biexponential function as shown in Fig. 4b using the following equation:

$$F(t) = A_1 \exp\left(\frac{t-B}{\tau_1}\right) + A_2 \exp\left(\frac{t-B}{\tau_2}\right),$$

where $F(t)$ is the time-dependent fluorescence intensity, A_i and B are the fitting parameters, and τ_i is the fluorescence lifetime, respectively. Each fitting parameter and lifetime is summarized in Table 1. The fluorescence decay is generally fitted by a single exponential form; in that case, we could quantify the energy transfer rate constant by using the lifetime and the quantum yield. However, the present plot cannot be fitted by such a simple function. The biexponential form would reflect the unique multiple relaxation processes existing in the single Ph-$(7T)_3$ molecule, with the quantitative analysis of the energy transfer in the dendrimer needing further investigation.

Conclusions

This study investigated the photochemical processes in a phenyl-core thiophene dendrimer. The broadband absorption of the dendrimer could be elucidated by quantum calculations of the absorption peaks of the moieties comprising it; this has been conceptualized as "multiple π-conjugations". Quantum calculations and absorption, PL, and excitation spectra were used to explain the unique light-energy transfer process. Light energy absorbed near the core was transferred to the dendrons, while being utilized for molecular vibrations and internal conversions, and finally emitted as long-wavelength PL. The fluorescence lifetime evaluation also suggested the existence of various relaxation processes in a single molecule. The results and methods (a combination of spectroscopy and quantum calculations for each part of the dendrimer) presented here could be used as an effective baseline to synthesize π-conjugated dendrimers with specific properties, which could guide the development of a new class of optoelectronic materials.

Author contributions

Mizuho Yamagishi: data curation; software; formal analysis; validation; investigation; visualization; methodology; writing-original draft; project administration; writing-review & editing. Shohei Horike: conceptualization; resources; software; formal analysis; funding acquisition; validation; investigation; visualization; methodology; writing-original draft; writing-review & editing. Yasuko Koshiba: resources; formal analysis; funding acquisition. Atsunori Mori: resources; validation; investigation. Kenji Ishida: conceptualization; resources; formal analysis; supervision; funding acquisition; methodology; writing-review & editing.

Conflicts of interest

There are no conflicts to declare.

Acknowledgements

The authors thank JST CREST and JSPS KAKENHI. S. H. would like to thank JST PRESTO. A part of this work was conducted in the Institute of Molecular Science (IMS) and was supported by the "Advanced Research Infrastructure for Materials and Nanotechnology in Japan (ARIM)" of the Ministry of Education, Culture, Sports, Science and Technology (MEXT). Proposal Number JPMXP1222MS1072.

References

1 G. M. Dykes, *J. Chem. Technol. Biotechnol.*, 2001, **76**, 903.
2 J. Hu, K. Hu and Y. Cheng, *Acta Biomater.*, 2016, **35**, 1.
3 M. L. Mansfield, *Polymer*, 1994, **35**, 1827.
4 Y. Cheng, L. Zhao, Y. Li and T. Xu, *Chem. Soc. Rev.*, 2011, **40**, 2673.
5 X. Ma, J. Tang, Y. Shen, M. Fan, H. Tang and M. Radosz, *J. Am. Chem. Soc.*, 2009, **131**, 14795.
6 S. Svenson and D. A. Tomalia, *Adv. Drug Delivery Rev.*, 2005, **57**, 2106.
7 M. E. Köse, W. J. Mitchell, N. Kopidakis, C. H. Chang, S. E. Shaheen, K. Kim and G. Rumbles, *J. Am. Chem. Soc.*, 2007, **129**, 14257.
8 W. J. Mitchell, N. Kopidakis, G. Rumbles, D. S. Ginley and S. E. Shaheen, *J. Mater. Chem.*, 2005, **15**, 4518.
9 E. R. Gillies and J. M. J. Fréchet, *Drug Discovery Today*, 2005, **10**, 35.
10 R. M. Crooks, M. Zhao, L. Sun, V. Chechik and L. K. Yeung, *Acc. Chem. Res.*, 2001, **34**, 181.
11 R. Duncan and L. Izzo, *Adv. Drug Delivery Rev.*, 2005, **57**, 2215.
12 D. Q. McNerny, P. R. Leroueil and J. R. Baker, *WIREs Nanomed. Nanobiotechnol.*, 2010, **2**, 249.
13 O. F. Khan, E. W. Zaia, S. Jhunjhunwala, W. Xue, W. Cai, D. S. Yun, C. M. Barnes, J. E. Dahlman, Y. Dong, J. M. Pelet, M. J. Webber, J. K. Tsosie, T. E. Jacks, R. Langer and D. G. Anderson, *Nano Lett.*, 2015, **15**, 3008.
14 M. Á. Ortega, A. G. Merino, O. F. Martínez, J. R. Ruiz, L. Pekarek, L. G. Guijarro, N. G. Honduvilla, M. Á. Mon, J. Buján and S. G. Gallego, *Pharmaceutics*, 2020, **12**, 874.
15 M. R. Carvalho, R. L. Reis and J. M. Oliveira, *J. Mater. Chem. B*, 2020, **8**, 1128.
16 A. Sharma and A. Kakkar, *Molecules*, 2015, **20**, 16987.
17 J. Li, H. Liang, J. Liu and Z. Wang, *Int. J. Pharm.*, 2018, **546**, 215.
18 Y. Jin, G. Huang, D. Han, P. Song, W. Tang, J. Bao, R. Li and Y. Liu, *Composites, Part A*, 2016, **86**, 9.
19 S. Chandra, M. D. Patel, H. Lang and D. Bahadur, *J. Power Sources*, 2015, **280**, 217.
20 S. Hata, Y. Yamaguchi, R. Nakata, K. Kametani, Y. Du, Y. Shiraishi and N. Toshima, *Diamond Relat. Mater.*, 2021, **120**, 108656.

21 A. K. Ilunga and R. Meijboom, *Catal. Lett.*, 2019, **149**, 84.

22 K. R. Raghupathi, J. Guo, O. Munkhbat, P. Rangadurai and S. Thayumanavan, *Acc. Chem. Res.*, 2014, **47**, 2200.

23 C. Devadoss, P. Bharathi and J. S. Moore, *J. Am. Chem. Soc.*, 1996, **118**, 9635.

24 D. L. Jiang and T. Aida, *Nature*, 1997, **388**, 454.

25 M. I. Ranasinghe, M. W. Hager, C. B. Gorman and T. Goodson III, *J. Phys. Chem. B*, 2004, **108**, 8543.

26 K. Shinbo, Y. Ikeda, C. Xia, K. Kato, F. Kaneko and R. C. Advincula, *Curr. Appl. Phys.*, 2005, **5**, 314.

27 G. Ramakrishna, A. Bhaskar, P. Bauerle and T. Goodson III, *J. Phys. Chem. A*, 2008, **112**, 2018.

28 K. Oki, S. Horike, M. Yamaguchi, C. Takechi, Y. Koshiba, T. Fukushima, A. Mori and K. Ishida, *Mol. Syst. Des. Eng.*, 2020, **5**, 809.

29 Y. Karpov, T. Erdmann, M. Stamm, U. Lappan, O. Guskova, M. Malanin, I. Raguzin, T. Beryozkina, V. Bakulev, F. Günther, S. Gemming, G. Seifert, M. Hambsch, S. Mannsfeld, B. Voit and A. Kiriy, *Macromolecules*, 2017, **50**, 914.

30 R. Kroon, D. Kiefer, D. Stegerer, L. Yu, M. Sommer and C. Müller, *Adv. Mater.*, 2017, **29**, 1700930.

31 O. Usluer, S. Demic, D. A. M. Egbe, E. Birckner, C. Tozlu, A. Pivrikas, A. M. Ramil and N. S. Sariciftci, *Adv. Funct. Mater.*, 2010, **20**, 4152.

32 W. W. H. Wong, C. Q. Ma, W. Pisula, C. Yan, X. Feng, D. J. Jones, K. Müllen, R. A. J. Janssen, P. Bäuerle and A. B. Holmes, *Chem. Mater.*, 2010, **22**, 457.

33 S. Tanaka, D. Tanaka, G. Tatsuta, K. Murakami, S. Tamba, A. Sugie and A. Mori, *Chem. – Eur. J.*, 2013, **19**, 1658.

34 R. A. Eittah and R. Hilal, *Bull. Chem. Soc. Jpn.*, 1976, **49**, 2158.

35 H. Chosrovian, S. Rentsch, D. Grebner, D. U. Dahm and E. Brickner, *Synth. Met.*, 1993, **60**, 23.

36 R. Colditz, D. Grebner, M. Helbig and S. Rentsch, *Chem. Phys.*, 1995, **201**, 309.

37 S. Bonardd, D. D. Díaz, A. Leiva and C. Saldías, *Polymers*, 2021, **13**, 4404.

38 O. Varnavski, I. D. W. Samuel, L.-O. Pålsson, R. Beavington, P. L. Burn and T. Goodson III, *J. Chem. Phys.*, 2002, **116**, 8893.

39 M. Cotlet, T. Vosch, S. Habuchi, T. Weil, K. Müllen, J. Hofkens and F. D. Schryver, *J. Am. Chem. Soc.*, 2005, **127**, 9760.

40 P. Ceroni, G. Bergamini, F. Marchioni and V. Balzani, *Prog. Polym. Sci.*, 2005, **30**, 453.

41 J. F. Galindo, E. Atas, A. Altan, D. G. Kuroda, S. F. Alberti, S. Tretiak, A. E. Roitberg and V. D. Kleiman, *J. Am. Chem. Soc.*, 2015, **137**, 11637.